Proposal for stochastic resonance in a ferroelectric-graphene transistor

Madhav Ramesh
School of Electrical and and Computer Engineering
Cornell University
Ithaca, USA
mr974@cornell.edu

Amit Verma
Dept. of Electrical Engineering
Indian Institute of Technology Kanpur
Kanpur, India
amitkver@iitk.ac.in

Arvind Ajoy
Dept. of Electrical Engineering
Indian Institute of Technology Palakkad
Palakkad, India
arvindajoy@iitpkd.ac.in

***Abstract*—Stochastic Resonance (SR) is a phenomenon involving non-linear systems, where the addition of noise improves some figure of measurement of the system – for example, power, signal-to-noise ratio, bit error rate. Ferroelectric materials possess a double-well energy landscape, which should enable them to be used for bi-stability based SR. However, measuring the polarization of a ferroelectric is difficult. This work proposes a design for a ferroelectric-graphene transistor. The drain current, which can be measured easily, then tracks the polarization of the ferroelectric. The choice of graphene as the channel material should ensure that the double-well nature of the energy landscape of the ferroelectric is preserved in the transistor. The choice of an n-type wide bandgap (WBG) contact should eliminate ambipolar conduction in the graphene transistor. Via numerical simulations, it is shown that the drain current of the transistor demonstrates SR while detecting weak but periodic signals. This work motivates experimental investigation of SR in ferroelectrics and ferroelectric-graphene transistors.**

***Index Terms*—Ferroelectric double well, stochastic resonance, graphene transistor**

I. Introduction

Stochastic Resonance (SR) describes the improvement in the figure of merit of a non-linear measurement system due to the addition of an optimal amount of noise. It is a counter-intuitive phenomenon, and is usually facilitated by the non-linearity of the system. SR was first proposed by Benzi et al. [1] to explain the quasi-periodic variation in atmospheric temperature over large time periods. It is interesting to note that SR has been discovered in biological systems as well – for example, the nervous systems of crayfish and paddlefish [2], [3] and the human auditory system [4].

Recently, several engineering applications of SR have emerged, such as a visual aid [5], a low power photodetector [6] and weak-signal detectors [7], [8]. The above applications are based on devices/systems whose non-linearity can be represented by a detection threshold $\pm V_c$, shown for example in Fig. 1. In such systems, the amplitude of the weak signal alone is lower than V_c, resulting in a zero output. However, the addition of an optimum amount of noise causes the weak input to cross the threshold, thereby enabling detection. Since the detector itself is biased in its *off* (below-threshold) state, such systems can be designed to consume very low power.

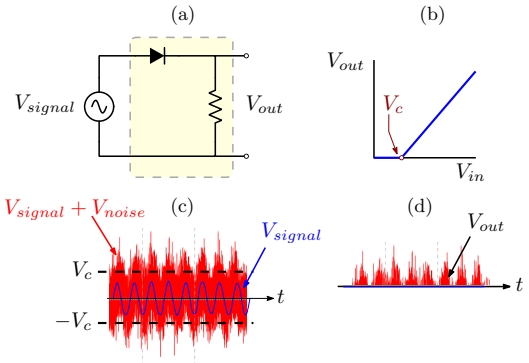

Fig. 1. Example of threshold based stochastic resonance (SR). (a) Non-linear circuit with an ideal diode. (b) $V_{out} - V_{in}$ characteristics. (c) Subthreshold signal and added white noise. (d) V_{signal} alone will give zero output. However, addition of white noise causes a non-zero V_{out} with envelope similar to V_{signal}.

Devices/systems with a non-linearity resulting from bistable behaviour (such as a Schmitt trigger comparator [9]) demonstrate more robust SR. Ferroelectrics are a class of materials which have an inherent, bistable polarization-voltage ($P-V$) hysteresis as shown in Fig. 2(a). This bistability arises from the double-well energy landscape (free energy vs. polarization) of the ferroelectric [10]. Harnessing this inherent bistability of ferroelectrics could result in highly-scaled SR detectors. Let V_c represent the coercive voltage of the ferroelectric. Without noise, sub-critical signals ($V_o < V_c$) cannot switch the polarization of the ferroelectric. However, provided an optimum amount of noise (Fig. 2(b,c)) is added, even sub-critical signals can cause the polarization to switch. Since this switching is synchronized with the signal, such systems can enable robust communication strategies in noisy environments, as shown in Fig. 2(d) for the case of frequency modulated transmission using frequency shift keying (FSK). The additional robustness in this type of SR is due to bistable systems having only two possible output states, similar in spirit to the advantages of

AA thanks SERB (Science and Engineering Research Board, Government of India) for support through MTR/2021/000823 and CRG/2022/008128. AV thanks SERB Early Career Research Award (Grant No. ECR/2018/001076) for supporting the SURGE internship of MR.

979-8-3503-2368-9/23/$31.00 ©2023 IEEE

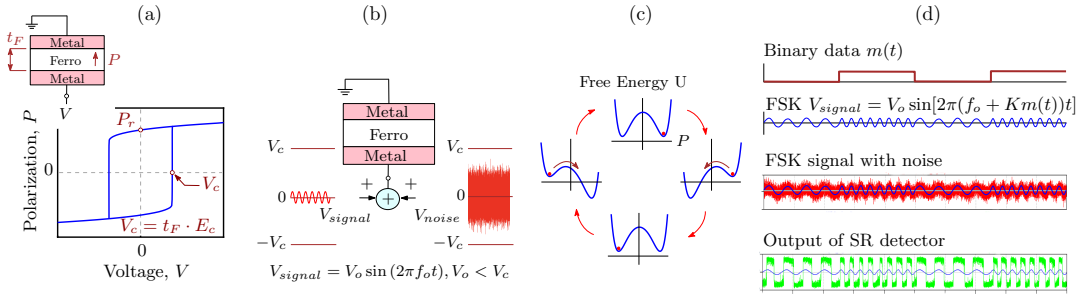

Fig. 2. Mechanism of bistablity based SR, shown using our simulations for a ferroelectric capacitor. (a) $P-V$ Hysteresis loop (b) Noise added to a weak periodic signal $V_o < V_c$ (c) The weak signal modifies the double well landscape of the ferroelectric, but does not eliminate the energy barrier. Noise cause the system to "jump" over the barrier and facilitates switching at the same frequency as the signal. (d) FSK communication in a noisy environment can benefit from bistable SR - the output of the SR detector robustly captures the frequency content of V_{signal}.

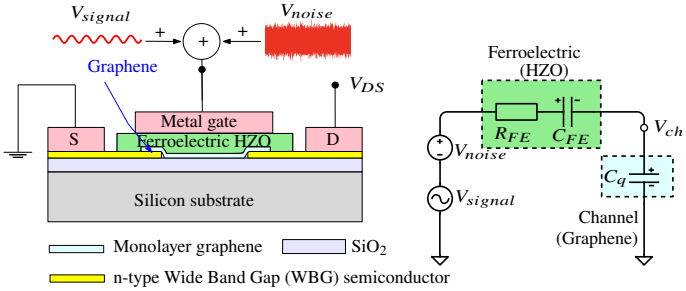

Fig. 3. Proposed ferroelectric-graphene transistor. The circuit diagram helps to determine the effective energy landscape and drain current.

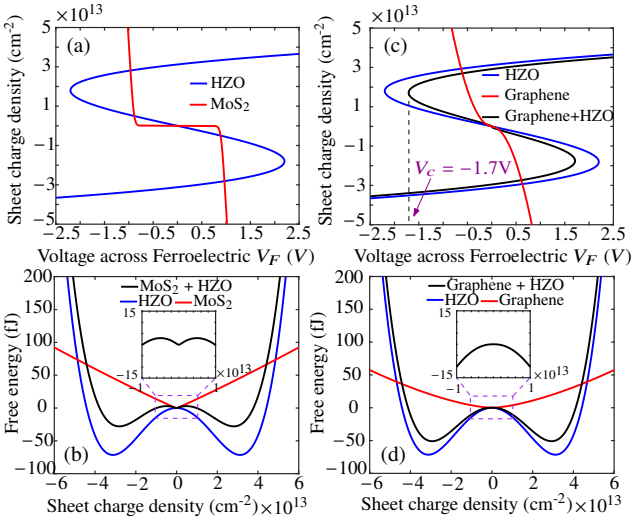

Fig. 4. Load-lines and the corresponding energy landscapes for MoS_2 (a,b) and graphene (c,d) in series with HZO. Note the double well landscape of the latter. The coercive voltage of the graphene-HZO combination is marked in (c).

digital communication over analog communication.

Measuring the polarization of a ferroelectric capacitor is non-trivial. Common techniques include Sawyer-tower circuits, current integration circuits using operational amplifiers [11] and optical methods [12]. However, all of these require either active circuit elements and other electrical components, or involve complex calculations. The aim of this work is to propose a transistor structure that can directly demonstrate SR in its current, due to a weak periodic voltage and noise at its gate terminal. For this, we propose a novel ferroelectric-graphene transistor (shown in Fig. 3) including two main innovations : (1) the channel is to be made from monolayer graphene (2) the contacts are to be made from a wide bandgap n-type material like SiC or MoS_2. The reasons for these design elements will be described in future sections. Due to its design, the drain current tracks the polarization of the ferroelectric. Via numerical simulations, we show that this structure should be able to detect weak signals through bistable SR.

II. Design of Ferroelectric-Graphene Transistor

A. Graphene as channel

As discussed in Fig. 2(c), a ferroelectric material (with thickness t_F) possesses a double well energy landscape given by $U = \alpha P^2 + \beta P^4 - PE$, with α, β being material properties and $E = V/t_F$ the electric field. This landscape generates the bistable behaviour seen in the hysteresis loop in Fig. 2(a). In order to enable SR, it is critical that the double well landscape is preserved when the ferroelectric is incorporated into a transistor. Our calculations reveal that the density of states (DOS) of the transistor channel determines the shape of the energy landscape in a ferroelectric transistor. The effect of finite graphene DOS on the channel charge can be represented by a quantum capacitance C_q as shown in the equivalent circuit of Fig. 3. The ferroelectric and the quantum capacitance of the channel are then equivalent to two non-linear capacitors in series. Using load-line analysis, an expression for the energy of this system is obtained [13]. The points where the load-lines intersect with the ferroelectric curve correspond to extrema in the energy landscape, as shown in Fig. 4. Note the load-line has been shifted (say using an appropriate metal workfunction) to make the energy landscape symmetric at zero DC gate voltage.

We assume the ferroelectric to be $Hf_{1-x}Zr_xO_2$ (HZO) with parameters as listed in Table I. Lets first consider a 2D channel material that has a bandgap, for example MoS_2 as shown in Fig. 4(a,b). Note the flat region that corresponds

TABLE I
HZO PARAMETERS FOR SIMULATIONS

Parameter	Value
Thickness t_F (nm)	20
α (mF^{-1})	-2.858×10^9
β $(m^5F^{-1}C^{-2})$	5.716×10^{11}
Resistivity ρ $(\Omega - m)$	30
Temperature T (K)	300
Area A_F (μm^2)	1

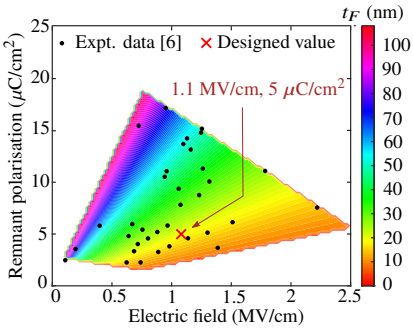

Fig. 5. Contour plot showing the minimum thickness t_F^* for a double well landscape, given different values of critical field (E_c) and remnant polarization (P_r) for ferroelectric HZO.

to the energy gap in MoS_2. Hence the load lines intersect at three points, corresponding to this heterostructure inevitably having five extrema (i.e three energy wells). This analysis is transferrable to any other semiconductor (2D or 3D) material with a bandgap as well. However, monolayer graphene does not have a bandgap. As a result, provided the thickness of the ferroelectric $t_F > t_F^* \equiv 1/2\alpha m$, the symmetry of the double-well energy landscape of the ferroelectric is essentially unaffected (see Fig. 4(c,d)). Only the value of the coercive voltage is altered. Here m is the slope of the graphene load-line near the origin.

Note α, β of a ferroelectric are related to its critical electric field (E_c) and remnant polarization (P_r), as $\alpha = -3\sqrt{3}E_c/4P_r$ and $\beta = 3\sqrt{3}E_c/8P_r^3$. Fig. 5 computes the effect of $\{E_c, P_r\}$ of HZO on the minimum thickness t_F^*

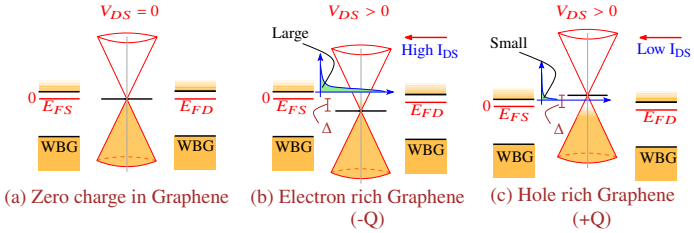

(a) Zero charge in Graphene (b) Electron rich Graphene (-Q) (c) Hole rich Graphene (+Q)

Fig. 6. Band-diagram to illustrate how the hole current in the device is suppressed. (a) Alignment when there is no charge in graphene. (b,c) Alignment for electron rich and hole rich graphene. The green region shows the product of the DOS in the channel with the electron distribution in the source, which is significantly lower in (c) as compared to (b), resulting in negligible current in the case of hole rich graphene. Note V_{DS} is assumed to be small in (b,c).

that ensures a double well landscape for a HZO-Graphene heterostructure. Note that our choice of t_F, α, β in Table I (corresponding to 20 nm, 1.1 MV/cm, 5 μC/cm^2) is well within the range of experimentally reported values of $\{E_c, P_r\}$ in Ref. [14].

B. Contact design for unipolar transport

If our transistor were to have ohmic contacts for both electrons and holes, then current flows from Drain→Source irrespective of whether the polarization state of the ferroelectric in positive or negative, making it impossible to observe SR (average current will be zero). Hence, we need to block the current due to one set of carriers (say holes). We propose using n-type wide bandgap (WBG) semiconducting contacts, similar to Ref. [15], [16] to suppress ambipolar conduction in the transistor, as shown in Fig. 6. When there is zero charge in the graphene channel and $V_{DS} = 0$, the Fermi levels E_{FS}, E_{FD} in the source, drain align with the Dirac point of the channel. The orange shading depicts the electron distribution as a function of energy. Note that the DOS in graphene is zero at the Dirac point, and grows linearly for energies above or below the Dirac point [17]. When the graphene channel is electron rich (charge -Q as in Fig. 6(b)), the Dirac point lies (say) Δ below E_{FS}. Assuming V_{DS} to be small, E_{FD} also lies above the Dirac point. The DOS in the channel near the conduction band edge of the source contact is high. The current is determined by the product of the DOS in the channel and the electron distribution in the source, depicted by the green inset. Hence, in the case of electron rich graphene, a high current flows from Drain→Source. For the same amount of hole charge (+Q) in the graphene channel (Fig. 6(c)), the Dirac point lies Δ above E_{FS}. Clearly, this alignment leads to a very small DOS in channel, and correspondingly low current from Drain→Source. The combination of n-type and wide bandgap of the contacts ensures that there is no current flow from the valence band of the contacts. With the above considerations, we thus assume the ideal case, where the small current in the case of hole rich graphene is approximately zero, and can be neglected.

C. Calculation of current due to stochastic input

The transistor model involves solving the following stochastic differential equation

$$\rho t_F \frac{dP}{dt} = V_{signal} + V_{noise} - (2\alpha P + 4\beta P^3) - V_{ch} \quad (1)$$

where V_{ch} is the channel voltage [17]. V_{signal} and V_{noise} represent the signal and noise (assumed white) voltages respectively. The method for solving Eq.(1) is similar to that available in literature [18]. Using a ballistic current model [19] and under the assumption of unipolar transport, we compute the current due to a weak periodic input in the presence of noise. We set the input signal $V_{signal} = 0.4\cos(2\pi \times 100\text{kHz} \times t)\text{V}$, with amplitude smaller than the coercive voltage of the Graphene-Ferroelectric heterostructure ($\sim$ 1.7V). Hence no switching is expected. However, using

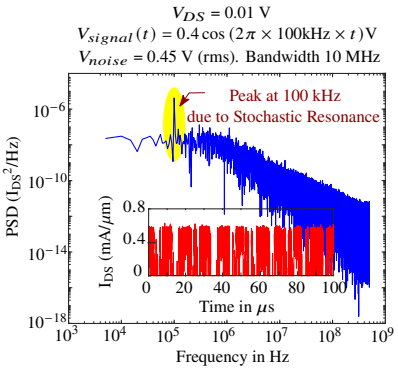

Fig. 7. SR using a current read-out. (Inset) Current I_{DS} switching over 100μs. The power spectral density (PSD) plot shows a peak at 100kHz, which is the frequency of the signal to be detected.

V_{noise} at 0.45 V_{rms} (limited to a 10 MHz bandwidth), the current switches quasi-periodically due to SR. This corresponds to a peak in the power spectral density at 100 kHz, as shown in Fig. 7.

III. Conclusion

In conclusion, we have proposed a ferroelectric-graphene transistor capable of demonstrating bistability based stochastic resonance. Our simulations suggest that the periodicity in the weak signal is captured and a direct current read-out can be obtained. The drain current of the proposed transistor tracks the polarization of the ferroelectric, which eliminates the need for other electrical or optical measurement techniques. We also demonstrate how graphene is superior to other semiconductors for the purpose of SR by virtue of its zero bandgap.

Acknowledgment

The authors gratefully acknowledge the use of the CHANDRA High Performance Computing cluster at IIT Palakkad.

References

[1] R. Benzi, G. Parisi, A. Sutera, and A. Vulpiani, "Stochastic resonance in climatic change," *Tellus*, vol. 34, no. 1, pp. 10–16, Feb. 1982.

[2] J. K. Douglass, L. Wilkens, E. Pantazelou, and F. Moss, "Noise enhancement of information transfer in crayfish mechanoreceptors by stochastic resonance," *Nature*, vol. 365, no. 6444, pp. 337–340, Sep. 1993.

[3] D. F. Russell, L. A. Wilkens, and F. Moss, "Use of behavioural stochastic resonance by paddle fish for feeding," *Nature*, vol. 402, no. 6759, pp. 291–294, 1999.

[4] A. Schilling, K. Tziridis, H. Schulze, and P. Krauss, "The Stochastic Resonance model of auditory perception: A unified explanation of tinnitus development, Zwicker tone illusion, and residual inhibition," *Prog. Brain Res.*, vol. 262, pp. 139–157, 2021.

[5] E. Itzcovich, M. Riani, and W. G. Sannita, "Stochastic resonance improves vision in the severely impaired," *Sci. Rep.*, vol. 7, no. 1, pp. 1–8, 2017.

[6] A. Dodda, A. Oberoi, A. Sebastian, T. H. Choudhury, J. M. Redwing, and S. Das, "Stochastic resonance in MoS_2 photodetector," *Nat. Commun.*, vol. 11, no. 1, pp. 1–11, 2020.

[7] S. Arai, W. Tamura, T. Yamazato, H. Hatano, M. Saito, H. Tanaka, and Y. Tadokoro, "Circuit Experiment of Photodiode-type Visible Light Communication Using the Stochastic Resonance Generated by Interfering Light Noise," in *Proc. Int. Symp. Circuits and Systems (ISCAS)*. IEEE, May 2021, pp. 1–5.

[8] Y. Hakamata, Y. Ohno, K. Maehashi, S. Kasai, K. Inoue, and K. Matsumoto, "Enhancement of weak-signal response based on stochastic resonance in carbon nanotube field-effect transistors," *J. Appl. Phys.*, vol. 108, no. 10, p. 104313, 2010.

[9] V. Melnikov, "Schmitt trigger: A solvable model of stochastic resonance," *Phys. Rev. E*, vol. 48, no. 4, p. 2481, 1993.

[10] M. Hoffmann, F. P. Fengler, M. Herzig, T. Mittmann, B. Max, U. Schroeder, R. Negrea, P. Lucian, S. Slesazeck, and T. Mikolajick, "Unveiling the double-well energy landscape in a ferroelectric layer," *Nature*, vol. 565, no. 7740, pp. 464–467, 2019.

[11] M. Stewart, M. G. Cain, and D. Hall, *Ferroelectric hysteresis measurement and analysis*. National Physical Laboratory Teddington, 1999.

[12] S. A. Denev, T. T. Lummen, E. Barnes, A. Kumar, and V. Gopalan, "Probing ferroelectrics using optical second harmonic generation," *J. Am. Ceram. Soc.*, vol. 94, no. 9, pp. 2699–2727, 2011.

[13] R. K. Jana, A. Ajoy, G. Snider, and D. Jena, "Transistor switches using active piezoelectric gate barriers," *IEEE J. Explor. Solid-State Comput. Devices*, vol. 1, pp. 35–42, 2015.

[14] M. Kobayashi, "A perspective on steep-subthreshold-slope negative-capacitance field-effect transistor," *Appl. Phys. Exp.*, vol. 11, no. 11, p. 110101, 2018.

[15] Y. Nagahisa and E. Tokumitsu, "Suppression of Hole Current in Graphene Transistors with N-Type Doped SiC Source/Drain Regions," in *Mat. Sci. Forum*, vol. 717. Trans. Tech. Publ., 2012, pp. 679–682.

[16] Y. Nagahisa, Y. Harada, and E. Tokumitsu, "Unipolar behavior in graphene-channel field-effect-transistors with n-type doped SiC source/drain regions," *Appl. Phys. Lett.*, vol. 103, no. 22, p. 223503, 2013.

[17] T. Fang, A. Konar, H. Xing, and D. Jena, "Carrier statistics and quantum capacitance of graphene sheets and ribbons," *Appl. Phys. Lett.*, vol. 91, no. 9, p. 092109, 2007.

[18] M. Ramesh, A. Verma, and A. Ajoy, "Kramers escape problem for white noise driven switching in ferroelectrics," *arXiv preprint arXiv:2112.01373*, 2021.

[19] S. O. Koswatta, A. Valdes-Garcia, M. B. Steiner, Y.-M. Lin, and P. Avouris, "Ultimate RF performance potential of carbon electronics," *IEEE Trans. Microw. Theory Tech*, vol. 59, no. 10, pp. 2739–2750, 2011.